Food Chemistry: X 12 (2021) 100142

Contents lists available at ScienceDirect

Food Chemistry: X

journal homepage: www.sciencedirect.com/journal/food-chemistry-x

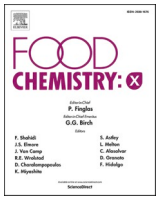

# Physical aspects of orange essential oil-contaning particles after vacuum spray drying processing

Fernanda de Melo Ramos, Vivaldo Silveira Júnior, Ana Silvia Prata *

*Department of Food Engineering, School of Food Engineering, State University of Campinas, P.O. Box 6121, 13083-862 Campinas, SP, Brazil*

ARTICLE INFO

*Keywords:*
Orange essential oil
Limonene
Encapsulation
Flavor
Vacuum

ABSTRACT

Vaccum spray drying has been shown as an alternative for drying sensitive compounds at lower temperatures than the conventional spray drying. Here, powders produced by both processes are compared considering their physical aspects and storage conditions. Orange essential oil-containing particles were produced by spray drying (190 °C/90 °C) and by vacuum spray drying (30 °C). The particles produced by vacuum spray dryer presented lower porosity and lower water adsorption than spray dried particles. Particles produced by both processes presented amorphous characteristics and no interaction between the wall material and encapsulated oil was observed. However, a lower oxidative stability during accelerated shelf life tests, in a period of 48 h, which can be related to the enhancement of oil retention. This study has significance for understanding the effect of the pressure and temperature over sensitive compounds and structural changes in the particles.

## Introduction

Brazil is the biggest producer of orange in the World, and an important byproduct of citrus processing is the orange essential oil (OEO). This aromatic oil is widely used as flavoring oil in beverages, baked goods, confectionery, perfumes, and cosmetics.

OEO is largely composed by the terpene d-limonene (90–96%) with small amounts of alcohols (0.8%), aldehydes (1.6%), esters (0.3%), and 1% of non-volatile compounds such as carotenoids, tocopherols, flavonoids, hydrocarbons, fatty acids and sterols (Gaffney, Havekotte, Jacobs, & Costa, 1996). The perception of flavor is a central driver that determines the sensory behavior of food products (Sobel, Gundlach, & Su, 2014). Despite aldehydes such as decanal, octanal, neral, geranial, citronellal, and others to be important to the characteristic orange flavor, terpenoids tend to be volatile and thermolabile, since they are especially prone to oxidative damage, chemical transformations, or polymerization reactions leading to the formation of unpleasant tastes and odors which also impairs over their shelf-life (Turek & Stintzing, 2013).

Thus, a central goal of flavor encapsulation is to prevent volatile losses and extend the shelf life of the products (Gouin, 2004; Reineccius, 2004). Spray drying encapsulation has been used as an effective way by the flavor and food industries to build a physical barrier against heat and oxygen exposition. It consists of the atomization of a coarse emulsion into a drying chamber at high temperatures, typically from 150 to 220 °C inlet air temperature (Phisut, 2012). In case specific of volatiles, improving the retention of core material in the final particle is very important, as much of these compounds can be lost during the process.

The process works based on selective diffusion and differences of vapor pressure between water and volatile compounds. Both aspects benefit the volatiles retention within the matrix (Sobel et al., 2014) even at such high temperatures. However, chemical reactions have exponential temperature-dependence (Atkins, 2002) and theoretically, a temperature rise of 10 °C approximately doubles the chemical reaction rates. Moreover, the presence of oxygen during spray drying contributes to autoxidation as well as hydroperoxide formation (Turek & Stintzing, 2013).

It is expected that the greatest damages to the compounds take place at the early stages of spray drying, before the formation of a dry crust at the surface of the atomized droplets (Reineccius, 1988). But losses also occur during drying, when the particle temperature reaches the boiling point of the water (King, 1995). Moreover, a high air inlet temperature can cause excessive evaporation and can result in cracks in the membrane inducing subsequent premature release and further degradation of the encapsulated ingredient (Zakarlan & King, 1982).

In this sense, vacuum spray drying (VSD) occurs at very low

* Corresponding author.
*E-mail addresses:* fernandalp29@hotmail.com, f153434@dac.unicamp.br (F.M. Ramos), vivaldo@unicamp.br (V. Silveira Júnior), asprata@unicamp.br (A.S. Prata).

https://doi.org/10.1016/j.fochx.2021.100142
Received 8 July 2021; Received in revised form 12 October 2021; Accepted 13 October 2021
Available online 15 October 2021

evaporation temperature and has been suggested as a new alternative to improve the retention of volatile molecules inside of the microparticles (Ramos, Oliveira, Soares, & Silveira Júnior, 2016; Ramos, Silveira Júnior, & Prata, 2019; Ramos, Ubbink, Silveira Júnior, & Prata, 2019). Other evidence about the feasibility of this type of process with sensitive compounds were also successfully reported in the literature (Islam et al., 2017; Islam, Kitamura, Yamano, & Kitamura, 2016; Semyonov, Ramon, & Shimoni, 2011) but it lacks a more deepened comprehension about the influence of process conditions in the protection provided by the particle.

Some questions arising from the use of this technique have been answered by our group during the development progress. Firstly, Ramos, Ubbink, et al., (2019) revealed that the vacuum conditions change the physical aspects of maltodextrin particles comparatively to those produced by conventional spray dryers, including the reduction of wettability time, which can be interesting for some applications, like those that need better dissolution in water (e.g. instantaneous beverages). Afterward, a thermal sensitive compound (OEO) was processed in the same system by Ramos, Silveira Júnior, et al., (2019) and similarly to that observed for maltodextrin, physical and morphological aspects from OEO-particles were changed. Moreover, the encapsulation efficiency of particles obtained by VSD was higher than SD, but the quality of the oil was not verified.

The aim of this work is to deepen the knowledge about the characteristics of particles achieved by VSD in order to properly retain and protect the active compound. The retention of limonene on microparticles was measured by gas chromatography and complementary analyses in the powder including porosity, water sorption, glass transition temperature, X-ray diffraction pattern, FTIR analysis, accelerated shelf-life test and its reconstitution ability in water were conducted for support the findings. This study has important implications to improve the development of this technology, broadening its application.

## Material and methods

### Material

The encapsulating matrix was composed of maltodextrin MOR-REX 1910 (Dextrose Equivalent (DE) = 9–12) and modified starch (Capsul), both kindly donated by Ingredion Brasil Ingredientes Industriais Ltd. (Mogi Guaçu, SP, Brazil). Cold pressed orange essential oil (CA 8028-48-6, density at 25 °C = 843 kg·m$^{-3}$, aldehydes = 1.11 %) was gently supplied by Citrosuco S/A Agroindustria (Matão, SP, Brazil). All other materials used in this work were of analytical grade.

### Methods

#### Emulsion preparation

Maltodextrin 24% (w/w) and modified starch 8% (w/w) were dispersed with distilled water and kept at approximately 25 °C for 24 h to ensure complete hydration of the polymers. The final wall material dispersion resulting from the blend of both polymers totalized 32 g of solids/100 g of solution. This formulation was based on the work previously described by Ramos, Silveira Júnior, et al., (2019). OEO was slowly added to the wall material dispersion under stirring at 20,000 rpm for 90 s using a homogenizer Ultra-Turrax IKA T18 basic (Wilmington, USA). OEO emulsion had a total solid concentration of 40 g/100 g, where the oily phase represents 20 g/100 g of the total solids (Charve & Reineccius, 2009; Jafari, Assadpoor, Bhandari, & He, 2008).

#### Particles formation

All encapsulation processes were carried out in the same chamber configuration and nozzle. A mini spray dryer MSD 1.0 (Labmaq do Brasil, Ribeirão Preto, Brazil) equipped with a two-fluid nozzle (Ø = 1.0 mm) and a peristaltic pump was employed with different conditions for each process as described below. All assays were performed in duplicate, whereas powder characterization analyses were made at least in triplicate.

*Spray drying process.* After stabilizing the inlet temperature at 190 °C, the conventional spray drying process (SD) was started. The outlet temperature was registered at 100 ± 5 °C. Fresh emulsion was fed at a 700 mL.h$^{-1}$ flow rate with 4 bar of atomizing pressure. The hot drying airflow rate was set at 81 m$^3$.h$^{-1}$ and the dried particles were collected at the collection vessel and the cyclone parts.

*Vacuum spray drying process.* The mini spray dryer was connected to vacuum pumps to keep pressure around 10–15 kPa during the process. A detailed description of the equipment can be found in Ramos, Ubbink, et al., (2019). After checking the sealed conditions for vacuum operation, fresh emulsion was fed at 60 mL.h$^{-1}$ without insertion of the hot air stream. Atomizing pressure was kept at 3 bar and its flow rate was set to 1.2 m$^3$.h$^{-1}$.

#### Powders analyses

*Retention of the volatile compounds encapsulated by SD and VSD processes.* The recovery of volatile compounds from pure OEO and microparticles was performed by liquid–liquid extraction using ethyl acetate (HPLC grade, Dinâmica, Diadema, Brazil). Approximately 0.5 g of sample was dissolved in deionized water (2.5 mL) and mixed for 30 s on vortex. After that, an aliquot of 0.5 mL of the reconstituted emulsion was mixed with 1.5 mL of ethyl acetate and further centrifuged (Biofuge Haemo Centrifuge, Heraeus Instruments, Apeldoorn, Netherlands) at 10,000 rpm for 10 min. This procedure was repeated twice after static resting of 16 h between the repetitions.

The analysis of the upper organic phase was conducted on a gas chromatograph system equipped with a flame ionization detector (GC-FID) (HP-7890, Agilent Technologies, Santa Clara, USA) coupled to an HP-5MS capillary column (J&W Scientific, 30 m length × 0.25 mm i.d. × 0.25 μm film thickness). An aliquot of the upper phase, free of water (1 μL) was injected in split mode (1:10) and the oven temperature was kept at 80 °C for 3 min, raised at 20 °C.min$^{-1}$ until 240 °C and held for 5 min. The temperatures of the injector and detector were set at 250 °C. Helium was used as the carrier gas (1.0 mL.min$^{-1}$). The standard compounds Limonene, myrcene, α-pinene, and linalool (purity ≥ 95%, Sigma-Aldrich, St. Louis, USA) were employed for helping the identification. Then, the retention times of the standards and the samples were compared. Calibration curves were built using *n*-decane as an internal standard for the quantification of volatiles.

The percentage of retention of volatile compounds (*RVC*) of each standard compound was calculated according to Equation (1):

$$RVC[\%] = \frac{RVC_{GC-FID}}{RVC_O} \quad (1)$$

where $RVC_{GC\text{-}FID}$ is the total volatile compounds quantified from the powder and $RVC_0$ is the total amount of RVC from OEO using a reference system that represent the initial concentration of oil and, therefore, volatile compounds. $RVC_{GC\text{-}FID}$ and $RVC_0$ were expressed as mg volatile compound/g powder.

*Inter-particle porosity ($\varepsilon_b$).* Porosity ($\varepsilon_b$) was calculated by determining the ratio of tapped bulk density ($\rho_b$) to particle true density ($\rho_t$) using Eq. (2) (Krokida & Maroulis, 1997):

$$\varepsilon_b = \left(1 - \frac{\rho_b}{\rho_t}\right) x100$$

*Tapped bulk density ($\rho_b$).* For the determination of tapped bulk density, approximately 2 g of powder was freely poured into a 50-mL glass graduated cylinder and the samples were repeatedly tapped manually until a negligible difference in height between succeeding

measurements was observed. Tapped bulk density was calculated as the ratio of the initial mass of powder (m) and its apparent (tapped) volume (V) and expressed as m/v ($g.cm^{-3}$) (Barbosa-Cánovas, Ortega-Rivas, Juliano, & Yan, 2005).

*Particle true density ($\rho_p$).* A gas pycnometer (AccuPyc 1330, Micromeritics Instrument Corporation, Norcross, GA, USA) was used to determine the particle true density of particles recovered by the SD and VSD processes under helium gas (99.995% purity). The temperature was maintained around 25 °C, and each sample was run 10 times.

*Water sorption isotherms.* Water sorption isotherms of OEO-containing microparticles were determined by the static gravimetric method at 25 °C. Approximately 0.5 g of sample was precisely weighed into small glass receptacles and placed in tightly closed recipients, with saturated saline solutions in distilled water for a given range of water activity at 25 °C (Supplementary material: Table S1). These recipients were placed in a temperature-controlled chamber at 25 ± 1 °C.

After stored, samples were regularly weighed on analytical balance at regular intervals until equilibrium was reached.

The experimental data obtained were adjusted by the Guggenheim–Anderson–de Boer (GAB) model, Eq. (3). The parameters of this model were determined through a non-linear regression analysis of the experimental data, using the Solver tool from Microsoft Excel software (Microsoft, Redmond, USA).

$$X_e = \frac{X_m C_{GAB} K_{GAB} a_w}{[(1 - K_{GAB} a_w)(1 - K_{GAB} a_w + C_{GAB} K_{GAB} a_w)]} \quad (3)$$

where: $X_e$ is the equilibrium moisture (g water/g dry solids); $X_m$ is the monolayer moisture content (g water/g dry solids); $a_w$ is the water activity (dimensionless); $C_{GAB}$ is a constant representing the adsorption on the first monolayer; $K_{GAB}$ is a constant representing the adsorption of molecules of water on multilayers.

*Glass transition temperature ($T_g$).* Samples equilibrated in each over saturated salt solution, as previously described in the 2.2.3.3 were weighted and sealed hermetically differential scanning calorimetry (DSC) aluminum pans. The mass of each sample pan was matched in advance with the mass of an empty reference pan to within ± 0.3 mg. Heating and cooling cycles were performed for each sample using a DSC 1 (Mettler Toledo, Schwerzenbach, Switzerland) acoording to the methods detailed in Supplementary material:Table S2.

The thermograms obtained were normalized based on the mass of the samples. The second scanning of each sample was performed to reduce the enthalpy relation of the amorphous powder, which appears in the first scan.

The glass transition temperature of a binary water–solid mixture depends on the plasticizing effects of the water and is described by the Gordon-Taylor model. The experimental data obtained were adjusted to this model (Eq. (4)).

$$T_g = \frac{Q_m . T_{g,m} + k_{GT} . Q_w . T_{g,w}}{Q_m + k_{GT} . Q_w} \quad (4)$$

where $T_g$, $T_{g,m}$, and $T_{g,w}$ are the glass transition temperatures of the water-containing system, anhydrous matrix and water, respectively, $Q_m$ is the solid conten, $Q_m$ is the water content on wet basis and $k_{GT}$ is the Gordon-Taylor coeficient. Glass transition temperature of pure water was taken as $T_{g,w} = -135$ °C.

*X-ray diffraction (XRD).* The X-ray diffraction analysis of the powders and wall materials was performed on a X-ray diffraction (ẌPert-MPD, Philips Analytical X-Ray, Almelo, Netherlands) using a graphite crystal monochromator with Cu-$K_{\alpha 1}$ filter radiation of $\lambda = 1.54056$ Å at 40 kV and 40 mA. The samples were analyzed in angles from 5° to 50° (2θ) with a step of 0.020° (0.02°.$s^{-1}$).

*Fourier transform infrared spectroscopy.* Fourier transform infrared spectroscopy (FTIR) was performed on the pure essential oil, the wall materials and microparticles produced. These measurements were made at 25 °C, in the range from 400 to 4000 $cm^{-1}$, using a spectrometer (IRPrestige-21, Shimadzu, Kyoto, Japan). The data were collected with the software IRSolution, version 1.60. For the analysis of the powder samples were prepared tablets in KBr while for the oil sample, the methodology used was the liquid film in KBr window.

*Accelerated shelf-life determination.* An Oxipres apparatus (Mikrolab Aarhus A/S, Højbjerg, Denmark) was employed to introduce higher pressure and temperature conditions to the microparticles and then, estimate the stability of these particles under stress conditions. The Oxipres method is based on oxygen consumption. The samples were placed inside a hermetically closed iron vessel and subjected to high oxygen pressure (5 bar) and kept at elevated temperature (60 °C). In this work, the particles were subjected under these stress conditions and evaluate in the periods of 24 and 48 h.

*Emulsions reconstitution.* Emulsion reconstitution was performed adding 20 mL of distilled water to 2.4 g of powder on Falcon tubes, based on the methodology of Drapala, Auty, Mulvihill, and O'Mahony (2017) with some modifications. The mixture was stirred in the vortex for 60 s for the complete dissolution of the powder. Then, samples were characterized for means of droplet size, optical microscopy, and kinetic stability, as described following.

*Droplet size distribution.* Dimensions of droplets in fresh emulsion reconstituted were measured by the light scattering technique using laser diffraction (Mastersizer Hydro 2000 MU, Malvern Instruments Ltd., Malvern, UK). The mean diameter was expressed as the volume-surface mean diameter $D_{[3,2]}$ (Sauter mean diameter Equation 5). The Span, which gives the width of size distribution, was calculated from Equation 6. The analysis was performed immediately after the emulsion reconstitution. Distilled water was used as dispersant medium and analysis was made at room temperature.

$$D_{[3,2]} = \frac{\sum n_i . D_i^3}{\sum n_i . D_i^2}$$

$$Span = \frac{(D_{0,9} - D_{0,1})}{D_{0,5}}$$

where $n_i$ is the number of droplets with diameter $D_i$, $D_{0,1}$, $D_{0,5}$ and, $D_{0,9}$ represent the diameter of accumulated distribution of 10%, 50% and 90% of total droplets, respectively.

*Optical microscopy.* Emulsions microstructure was visualized using an optical microscope (Axio Scope A1, Carl Zeiss, Gottingen, Germany). Images were taken with a 400x magnification (10x and 40x for ocular and objective lenses, respectively) immediately after the reconstitution. The software Axio Vision Rel. 4.8 was used for image acquisition.

*Kinetic stability.* The stability of reconstituted emulsion was evaluated immediately after resuspension and measurements performed for 24 h at 1-hour intervals by laser backscattering scanning technique using the Turbiscan Lab® Expert (Formulaction, I'Union, France).

*Statistical analysis.* The data were statistically analyzed by Tukey's test using the Statistica® software (Statsoft, Tulsa, Okla., USA). Differences between means were considered significant at a 95% confidence level ($p \leq 0.05$).

## Results and discussion

Physical and chemical aspects from particles are of utmost importance for technological applications and also to give insights about the oil quality. Particles produced by the conventional process and under vacuum conditions were characterized regarding both aspects.

*Oil retention dependent on processing conditions*

OEO used as the active compound was preliminary characterized (complete data not shown). Limonene contributes to 93.78 ± 3.74 g from each 100 g of oil. Myrcene (1.93 ± 0.08 g), α-pinene (0.39 ± 0.01 g), and linalool (0.32 ± 0.01 g) totalize 96.42% of the original OEO (Fig. 1). After elution of linalool, a total of 3.16% of compounds were eluted. The cold- pressed citrus oil contains about 90–95% of terpenes which in general oxidize readily in the air with the development of unpleasant flavors. Naturally occurring oxygenated compounds such as decanal, ocatanal, neral and geranial are included in these small percentages and they are primarily responsible for characteristic citrus flavor. For this reason, some process remove a portion of the terpenes which also increase its stability and solubility (Vora, Matthews, Crandall, & Cook, 1983).

When assessing the efficiency of a new technique of microencapsulation it is important to evaluate the retention of the active compound into the encapsulating system. Experiments in the conventional spray dryer (P = 1 atm; inlet temperature = 190 °C) were performed and the same equipment was operated under vacuum (P = 0.1–0.15 atm; internal temperature = 30 °C) to obtain OEO-containing dried particles. In general, the content of heat-sensitive compounds decreases with increasing temperature due to thermal and oxidative degradation (Shishir & Chen, 2017). Then, processing conditions, specifically temperature and airflow, straightly affect oil retention, as degradation products or any other sort of loss can be induced by these factors.

The chromatogram shown in Fig. 1 overlaps the original OEO, and the OEO extracted from particles obtained by SD and VSD. They were built using the same amount of sample from both microparticles, immediately after production. The results show the maintenance of the general profile of the components verified in the original oil, with no preferential losses of some compound. This result is expected since OEO contains minor compounds with a narrow range of vapor pressure and molecular size.

However, this chromatogram also shows some differences between the oil composition from SD and VSD particles. The amount of compounds in the OEO was determined by the area from GC-FID, and the standard curves obtained with the isolated compounds α-pinene, myrcene, limonene, linalool which represent the main compounds of the OEO. The relative quantity of the compounds after extraction from particles to the same amount of free OEO injected was then calculated as retention of the compound inside particles (Table 1).

We found that the VSD microparticles had the highest retention of limonene as well as some minor compounds. Since limonene represents the main compound of OEO, it was used as the target compound. Values of retention higher than the one originally added to the formulation (>100%) also were observed in other works (Consoli, Dias, Carvalho, Silva, & Hubinger, 2019). The limonene load was 166.6695 mg volatile/g of SD-powder and 209.4912 mg volatile/g of VSD-powder.

Losses of volatiles components in concentrated matrices are determined by their internal diffusional transport rather than their vapor pressure. This latter can occur in the early stage of drying when the oil is directly exposed to the air. Since limonene presents a volatilization temperature of 176.5 °C at 1 atm, we expect some losses in the atomization nozzle. In this region, the temperature is the highest and the crust is not yet formed, in a manner that the vapor pressure of the compound will control the losses instead of the diffusion coefficient after the matrix formation.

If on the one hand the high temperatures used in SD contributes to quickly form the surface crust, on the other, in VSD, the reduction of total pressure increases the differences between external temperature and temperature of volatilization of compounds. At reduced pressure, specifically 0.3 atm, the volatilization of free limonene takes place at 109.7 °C, a still high temperature compared to the drying conditions adopted inside VSD, resulting in the highest retention for these particles.

The previous work of Ramos, Silveira Júnior, et al., (2019) based on the macroscopic characterization of the powder suggests that there may be temporal differences for the superficial crust formation during VSD operation. The most likely reason for this correlation was that the driving force is very small. Here, we observe that even if the crust is not formed, the temperature of volatilization that still would determine the main losses is very superior to the evaporation temperature.

In conclusion, the high temperature employed to produce microparticles by SD should be considered the principal reason for volatiles loss in this sample, as the temperature could have induced the thermosensitive compounds volatilization during the atomization. Indeed, the VSD process is conducted at very low temperature and airflow, which represents more propitious conditions for volatile compounds preservation. Chen, Zhong, Wen, McGillivray, and Quek (2013) assessed the retention of limonene encapsulated with whey protein isolate (WPI) and soluble corn fiber by spray drying technique. The authors observed retention values equal to 81 ± 3% using the conventional process. According to the authors, the decrease in limonene levels reflected in the overall loss of volatile fraction in the powders during spray drying, most probably through oxidation or evaporation.

These findings are expected to have importance in a broad range of fields, influencing the further development of VSD technologies and improvements in formulations for conventional SD.

*Oil losses during storage*

The volatile losses also occur during storage, as they are dependent

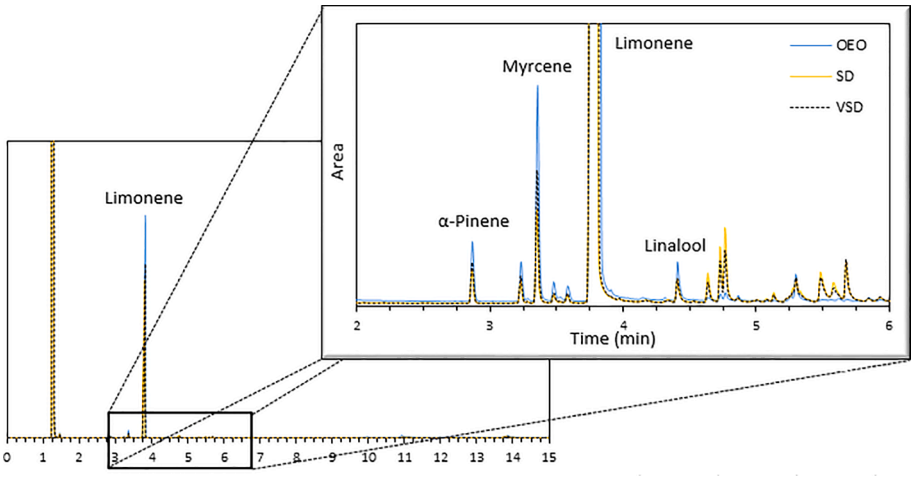


**Fig. 1.** Chromatograms of OEO extracted from particles obtained by SD and VSD.

**Table 1**
Mean and standard deviation values for limonene content, tapped bulk and particle true densities and inter-particle porosity for the microparticles.

| Sample | Limonene | | Tapped bulk density ($g \cdot mL^{-1}$) | Particle true density ($g \cdot mL^{-1}$) | Inter-particle porosity (%) |
|---|---|---|---|---|---|
| | Retention (%) | Loading (mg/g powder) | | | |
| SD-powder | $88.9^{a} \pm 2.7$ | $166.7^{a} \pm 5.0$ | $0.273^{a} \pm 0.006$ | $1.069^{a} \pm 0.030$ | $74.4^{b} \pm 0.9$ |
| VSD-powder | $111.7^{b} \pm 5.1$ | $209.5^{b} \pm 9.5$ | $0.347^{b} \pm 0.010$ | $1.131^{b} \pm 0.001$ | $69.3^{a} \pm 0.9$ |

Values are averages of two experiments, with each individual sample analyzed in triplicate. Different lowercase letters in the same column represent statistically significant differences ($p \leq 0.05$).

on the quality of the barrier formed by the particle. The barrier, or permeability of the shell, is relative to the structuration and the viscosity of the concentrated matrix, but also the morphological aspects such as size, shape, thickness of shell, oil droplets distribution.

Without considering the formulation, responsible by the internal diffusion and shell flexibility during particle formation, morphological aspects, as well as physical properties, are determined by mass and heat transfer rate during drying. Significantly differences in size distribution and morphology were verified between SD and VSD particles (Ramos, Silveira Júnior, et al., 2019). We would like to focus on the consequence of these differences for oil retention, rather than the cause of morphological differences, which has been covered by the authors. Then, physical characterization contributes to understanding the influence of the microparticle design and of the drying conditions in preserving the thermal-sensitive compound.

*Physical contribution: Inter-particle porosity ($\mathcal{E}_b$)*

Tapped bulk density (also known as bed density) considers the void spaces between the particles and refers to the ability of the bed of particles to be packed. This property is important for the commercialization of powdered products (packaging and shipping) (Quispe-Condori, Saldaña, & Temelli, 2011) and gives the compressibility index when from it subtracted the bulk density. These results are presented in Table 1.

The average tapped bulk density was 0.27 $g \cdot mL^{-1}$ for SD and 0.34 $g \cdot mL^{-1}$ for VSD particles. The microcapsules produced at higher temperature showed the lowest tapped bulk density, probably because of the faster drying, which results in a larger volume (and size). In fact, as the crust is quickly formed, the increased solid content at the surface does not let the moisture to evaporate, so that the increased internal pressure of particles inside causes a ballooning effect (Bhandari, Dumoulin, Richard, Noleau, & Lebert, 1992; Nijdam & Langrish, 2006). This effect forces the matrix/oil to be concentrated in the outer surface forming a vacuole. These structures are well represented in the literature, more dependent of the temperature, and of the design of spray dryer than from the formulation. Similar inflate/vacuole structures were reported in the microencapsulation of flaxseed oil by spray drying (Tonon, Grosso, & Hubinger, 2011) and in the spray drying of tomato pulp (Goula, Adamopoulos, & Kazakis, 2004).

The particle size distribution also could contribute to the packing density but there was reported to be similar for both particles (bimodal distribution with polydispersity values of 2.08 and 2.03 for SD and VSD respectively) (Ramos, Silveira Júnior, et al., 2019).

The particle true density, obtained from the adsorption of helium to the particles's surface through the opened pores, does not consider the spaces present inter and intra-particles. Similarly to tapped bulk density, the maximum true density was obtained with VSD powder (Table 1) which led to lower bed porosity (69.27%) than SD particles (74.37%). Orange juice powders produced in VSD by Islam et al. (2017) presented higher bed porosity, which ranged from 86.30 to 86.69%.

Porosity can present a direct relationship with the shelf life of dry products. A high porosity value indicates that much space remains between the particles and more occluded air within the particles, increasing the probability for degradation reactions and consequently reducing storage stability of products susceptible to oxidation (Reineccius, 2001; Tonon et al., 2011).

Considering the higher bed porosity as well as the concentration of matrix/oil in the outer surface (ballooning effect), it is reasonable to expect higher losses of volatiles in SD than in the VSD sample.

*Structural contribution*

In addition to the greater contact with oxygen that can affect the shelf life of the encapsulated oil, the structure of the concentrated matrix can modify the water sorption, which is also associated with changes in the stability of the material. Increased adsorbed water, decreases the viscosity of the concentrated phase and increases the mobility of the dispersed components. Water sorption isotherms data are used to predict the best storage conditions for maintaining extended shelf life of products, to calculate drying time, and for selection of packaging materials which is very important in the case of powdered products (Lomauro, Bakshi, & Labuza, 1985).

Sorption isotherms are mainly dependent on the formulation but some works reported that different structures can change the water sorption. Goula, Karapantsios, Achilias, and Adamopoulos (2008) compared their experimental data of tomato pulp processed by spray drying with freeze dried tomato pulp from Giovanelli, Zanoni, Lavelli, and Nani (2002). The work reported higher water uptake for spray dried powder as consequence of processing conditions.

The glass transition temperature ($T_g$), temperature at which an amorphous system changes from the glassy to the rubbery state, can be considered as a reference parameter to characterize the properties like quality and stability of food systems. When amorphous food powders are stored at temperatures above the $T_g$, structural alterations such as stickiness, caking, agglomeration and crystallization can occur (Kurozawa, Park, & Hubinger, 2009). The combination of sorption moisture data with glass transition temperature of sample was suggested by (Roos, 1993) in order to evaluate food stability and to obtain the critical values for the water activity and moisture content. Fig. 2 shows the curves of sorption isotherms and glass transition temperature curve for SD and VSD powders as function of water activity equilibrated under several humidity relatives at 25 °C. The water content and $T_g$ values were fitted by the GAB and Gordon-Taylor models, respectively, and the predicted parameters of the fitted GAB model to the experimental data for sorption isotherm of SD and VSD orange essential oil powders are also depicted in Fig. 2. The glass transition temperature for both samples were similar. Also, both materials presented sigmoidal shape isotherms (Type II) which is characteristic of porous materials. However, the powders produced by VSD showed sorption isotherm slightly below to the samples produced by the conventional process most likely due to their compact powder. Therefore, the equilibrium moisture reached for SD particles is higher than that obtained for VSD particles. The lower inter-particle porosity (Table 1) of the VSD particles engenders smaller transfer area and consequently lower water adsorption. Besides, the harsh conditions during the spray drying can result in formation of cracks due to extreme drying affecting the moisture transport.

The parameters of GAB model, shown in Fig. 2, confirm these findings. Lewicki (1997) reported that the values C and K should assume ranges from $5.67 \leq C < \infty$ and $0.24 \leq K \leq 1$, and assures that the calculated monolayer moisture content ($X_m$) values differ by not more than ± 15.5% from the true monolayer capacity. The results obtained for OEO microcapsules are within the ranges specified by the author indicating that the model correctly described the water adsorption isotherms.

| Powder | $X_m$ (g water/ g dry matter) | C | K | E |
|---|---|---|---|---|
| **SD** | 0.0775 | 34.64 | 0.72 | 12.38 |
| **VSD** | 0.0599 | 34.41 | 0.76 | 11.67 |

Where: E is relative mean error.

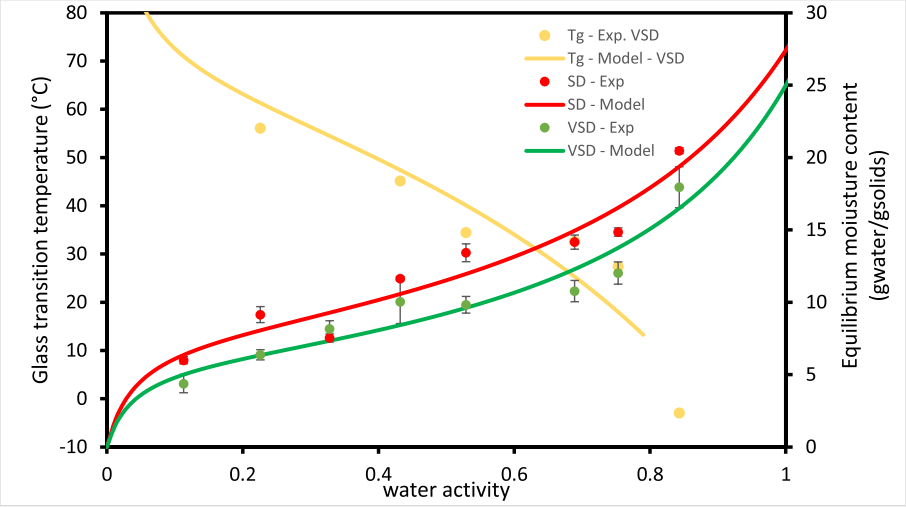


**Fig. 2.** Glass transition temperature (Tg) and equilibrium moisture content (EMC), adjusted using the Gordon-Taylor and GAB models, respectively, as function of the water activity ($a_w$) for spray dried and vacuum spray dried powder at 25 °C.

The GAB model is based on the monolayer moisture ($X_m$) concept and provides this value considered as safe moisture for dried foods (Tonon et al., 2009). For VSD powders, the value of the amount of water strongly adsorbed in the powders was 0.0599 g water/g dry matter, whereas for the sample produced at high temperature the $X_m$ value was 0.0775 g water/g dry matter, both at a storage temperature of 25 °C. Values of monolayer moisture ranging from 0.0354 to 0.0403 g water/g dry matter (Islam et al., 2016) and 0.049–0.091 g water/g dry matter

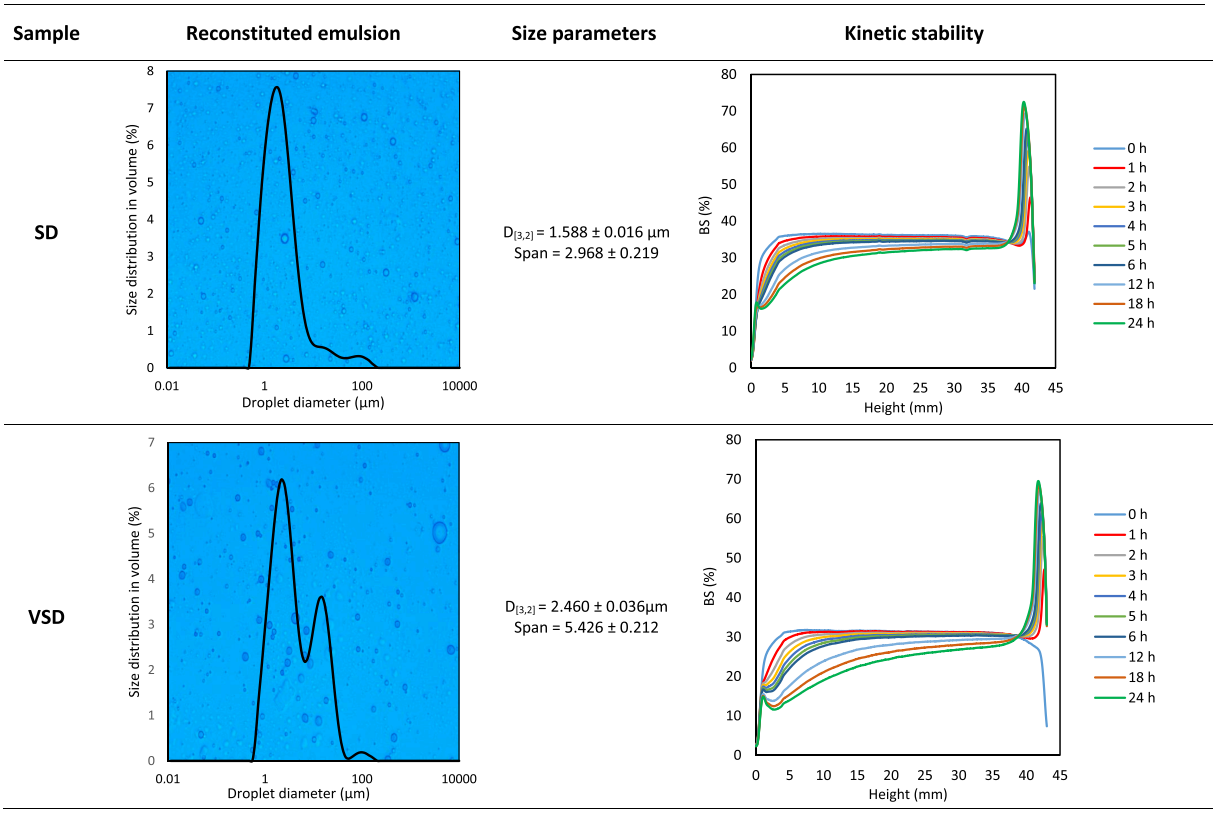


**Fig. 3.** Droplet size distribution coupled with micrographs, size parameters and backscattering profiles obtained for the reconstituted emulsions.

(Islam et al., 2017) using GAB model, were found for orange juice powder produced by vacuum spray drying.

The lower critical moisture content indicates the vulnerability of the VSD powder under the storage conditions. The rubbery state is characterized by the lower viscosity than the glassy region, which contributes to the higher water mobility for degradation reactions. However, with the lower viscosity, there is a probability of oil droplets moving and coalesce during storage. Resuspension of the powders in distilled water for emulsion reconstitution allows the assessment of the ability of an emulsion in preserve the original characteristics of the colloidal system. Resuspension tests were conducted after 6 months of storage at 25 °C, in samples stored in flasks inside a desiccator containing silica, to confirm this hypothesis. The moisture content and water activity of powders were, respectively, 1.3%, 0.13 for SD particles and, 6.27%, 0.41 for VSD particles (Ramos, Silveira Júnior, et al., 2019). The distribution size charts, micrographs, size parameters and backscattering profiles of the reconstituted emulsions by the two processes are represented in Fig. 3. As can be seen by these data, both powdered samples were not able to keep the original size of the emulsion fed into the dryers ($D_{[3,2]} = 0.913$ μm; Ramos, Silveira Júnior, et al. (2019)), but, the droplet size of SD emulsion ($D_{[3,2]} = 1.588$ μm) was closer to original emulsion. The comparative size distribution between SD and VSD in the Fig. 3, evidenciate a new peak formed for VSD particles, probably due to coalesced droplets, which increased the mean size of the VSD emulsion.

The stability of the colloidal system is dependent on the emulsion droplet size. The increased sizes provided decreased stability to the emulsions evaluated by backscattering (BS) profiles when compared to original emulsion (Ramos, Silveira Júnior, et al., 2019). Immediately after the homogenization process (t = 0 h), BS values were constant for both samples. However, the destabilization mechanism by creaming characterized by the trend of reduction of BS values in the inferior zone of the measuring cell and a rise of these values at the top of the cell was observed over time, for all samples. For VSD emulsion, the destabilization showed to be more pronounced than SD emulsion over time. After 24 h, the droplets that initially were dispersed homogeneously in the emulsified system turned more concentrated at top measuring cell promoting the increase of BS values, whereas minors values could be observed in the bottom-measuring cell.

An accelerated oxidation test was performed to evaluate the barrier properties of both particles. Specific conditions of pressure and temperature adopted (see Section "*Accelerated shelf-life determination*") represent two distinct storage periods. In Fig. 4, the curves did not present a well-defined inflection point for the induction time. After a period of 24 h, both particles presented similar behavior with a mild drop of pressure. However, after 48 h, the particles present distinct behavior in the oil protection. SD microparticles had better performance of accelerated oxidative stability in relation to the samples obtained under vacuum, verified by the faster pressure drop over time (Fig. 4b).

As the fat oxidizes it consumes the oxygen present in the vessel dropping their internal pressure. Then, the higher oxidation in VSD particles at 48 h can be due to the higher exposition of oil content of these particles and, consequently the enhanced oxidative stability in the SD powders can be attributed to the lower amount of retained volatiles compounds (Table 1).

Despite the physical structure change the ability of the powders to adsorb water, the different processes (VSD and SD) were not able to change their molecular structure. X-ray diffractogram for the OEO microparticles as well for the pure maltodextrin and modified starch are showed in Fig. 5A. XRD profiles showed that both microparticles presented amorphous structure based on the occurrence of large diffuse peaks (broadband). The XRD profile of OEO-microparticles was similar to the results reported by Cano-Chauca, Stringheta, Ramos, and Cal-Vidal (2005) for the particles formed by system mango juice and maltodextrin 20 DE. The maltodextrin also has amorphous characteristics as can be confirmed by Fig. 5. As expected, the modified starch showed a diffraction profile characteristic of semi-crystalline structures. The crystalline region is exclusively associated with the double helix arrangement of amylopectin, while the amorphous region can be largely attributed to amylose (Zobel, 1988). However, after the processes the crystalline region it disappeared. Similar behavior for XRD profile for modified starch was reported by Silva, Azevedo, Cunha, Hubinger, and Meireles (2016).

In general, the samples coming from spray drying process exhibit amorphous structures favoring the imprisonment of components in the matrix (Jansen-Alves et al., 2019) when glassy amorphous.

FTIR analysis was used for assessed qualitatively the compatibility of the encapsulated oil with the biopolymers and to know if some change in the spectrum of microparticles was made by the different drying processes. According to Baranauskiene, Venskutonis, Dewettinck, and Verhé (2006) when natural flavorings are encapsulated by different structures, it is important to know what changes in composition are occurring during emulsification and, in specific, during spray drying process.

Fig. 5B shows the spectra of all components applied in the

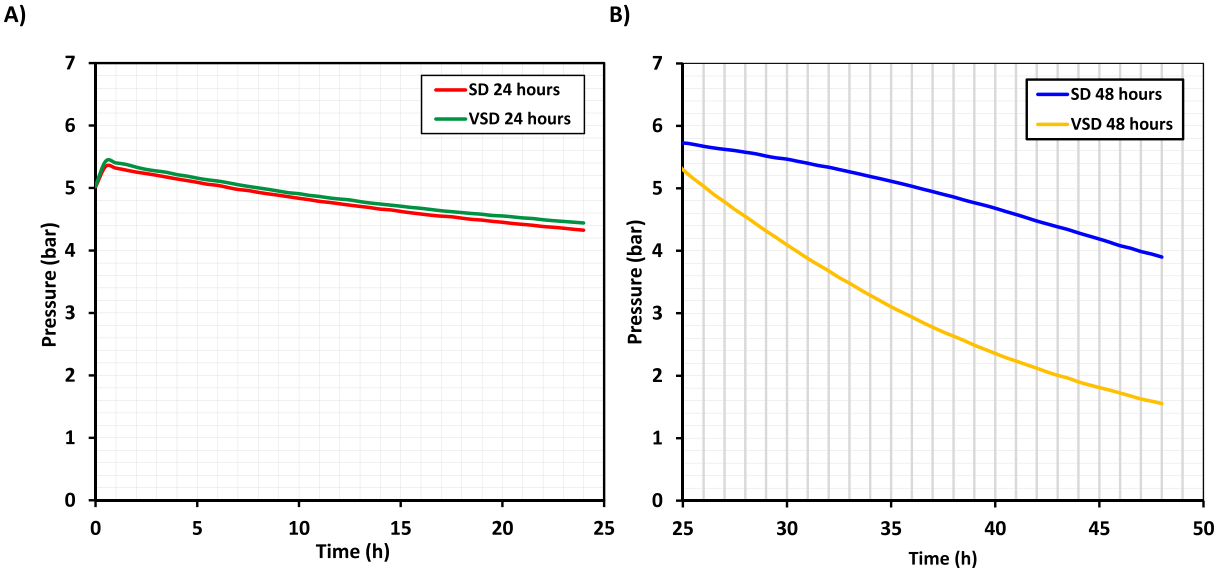


**Fig. 4.** Effect of the pressure and temperature over particle stability: (A) 24 h; (B) 48 h.

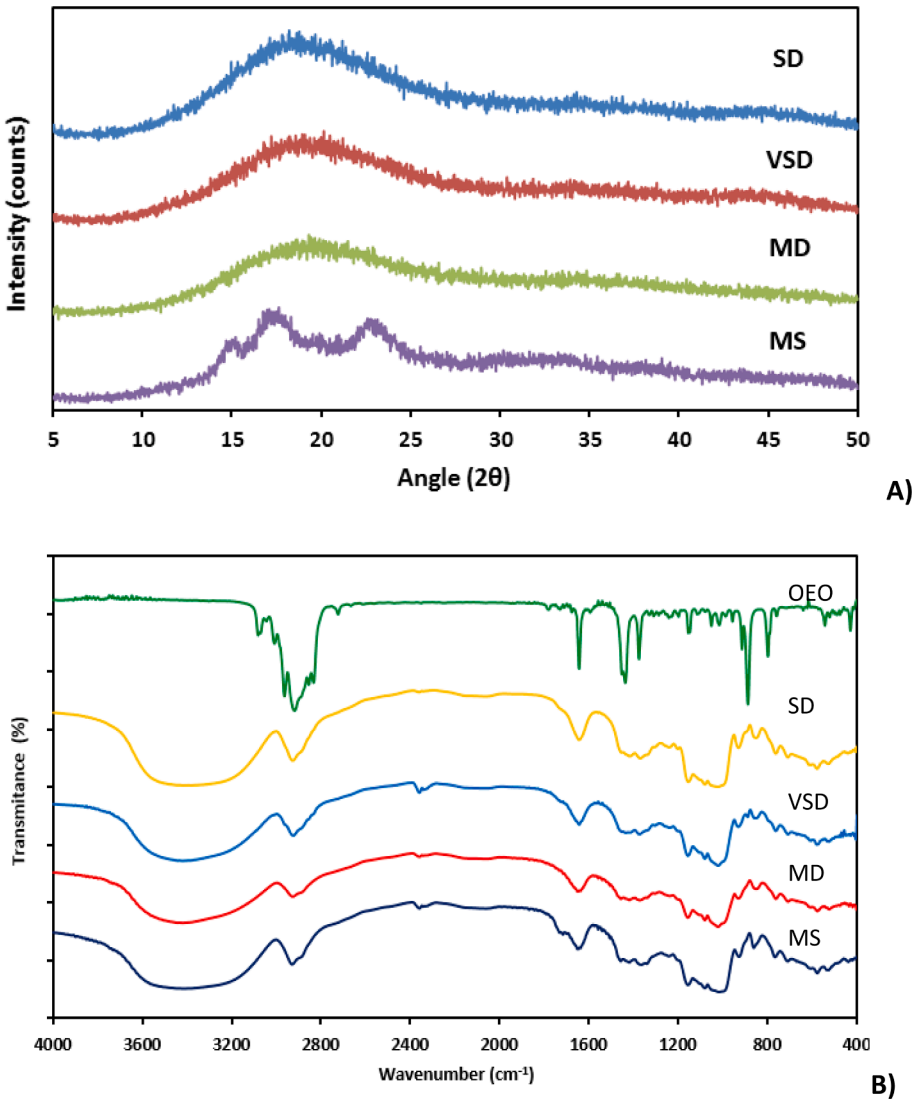


**Fig. 5.** X-ray diffractogram (A) and FTIR spectra for the microparticles produced by SD and VSD and materials used in the formulation of the emulsion. MD: maltodextrin; MS: modified starch; OEO: orange essential oil.

microencapsulation process as well as of the encapsulated oil from different processes. The profile shown for OEO microcapsules exhibited very similar FTIR spectrum when compared with matrices used. The different processes did not affect the FTIR spectra of the VSD and SD powders. The amount of aroma compound present in the matrix polymeric is insufficient to modify the behavior of the OEO microparticles. Besides that, chemical interaction between oil and biopolymers in the structure of the microcapsule was not observed, evidenced by the absence of formation of new bands.

## Conclusion

The results obtained in this study indicate that the under milder drying conditions employed on VSD allows a retention of volatiles molecules enhanced. Particles achieved at reduced pressure had higher tapped bulk and particle true densities, and thus lower inter-particle porosity, which is desirable during the store mainly of oxidizable compounds by providing greater protection against degradation reactions. This lower porosity results in a smaller transfer area, which explains the lowest water adsorption by the particles, achieved under vacuum. It is suggested that the higher oxidation in VSD particles at 48 h can be due to higher oil content in these particles. The enhancement of retention of oil reduced the oxidative stability of this sample. This work also verified that the encapsulation of orange essential oil by both processes did not demonstrated interaction between wall material and encapsulated oil as confirmed by FTIR analysis and that all particles produced presented amorphous characteristics. Therefore, preservation of thermo-sensitive components in particulates obtained by spray drying can be improved by the use of vacuum in the process.

## Declaration of Competing Interest

The authors declare that they have no known competing financial interests or personal relationships that could have appeared to influence the work reported in this paper.

*Acknowledgements*

The authors thank for the scholarship of the first author CAPES (Coordenação de Aperfeiçoamento de Pessoal de Nível Superior, Brazil), Finance Code 001, and for the financial support provided by Fapesp (Fundação de Amparo à Pesquisa do Estado de São Paulo) in the Project 2016/09824-4.

## Appendix A. Supplementary data

Supplementary data to this article can be found online at https://doi.org/10.1016/j.fochx.2021.100142.

## References


Atkins, P. W. (2002). *Kurzlehrbuch physikalische chemie* (3rd ed.). Weinheim, Germany: Wiley-VCH.

Baranauskiene, R., Venskutonis, P. R., Dewettinck, K., & Verhé, R. (2006). Properties of oregano (Origanum vulgare L.), citronella (Cymbopogon nardus G.) and marjoram (Majorana hortensis L.) flavors encapsulated into milk protein-based matrices. *Food Research International, 39*(4), 413–425. https://doi.org/10.1016/j.foodres.2005.09.005

Barbosa-Cánovas, G. V., Ortega-Rivas, E., Juliano, P., & Yan, H. (2005). *Food Powders: Physical Properties, Processing.* New York: Plenum Publishers.

Bhandari, B. R., Dumoulin, E. D., Richard, H. M. J., Noleau, I., & Lebert, A. M. (1992). Flavor encapsulation by spray drying: Application to citral and linalyl acetate. *Journal of Food Science, 57*(1), 217–221. https://doi.org/10.1080/87559128909540848

Cano-Chauca, M., Stringheta, P. C., Ramos, A. M., & Cal-Vidal, J. (2005). Effect of the carriers on the microstructure of mango powder obtained by spray drying and its functional characterization. *Innovative Food Science & Emerging Technologies, 6*(4), 420–428. https://doi.org/10.1016/j.ifset.2005.05.003

Charve, J., & Reineccius, G. A. (2009). Encapsulation performance of proteins and traditional materials for spray dried flavors. *Journal of Agricultural and Food Chemistry, 57*(6), 2486–2492. https://doi.org/10.1021/jf803365t

Chen, Q., Zhong, F., Wen, J., McGillivray, D., & Quek, S. Y. (2013). Properties and stability of spray-dried and freeze-dried microcapsules co-encapsulated with fish oil, phytosterol esters, and limonene. *Drying Technology, 31*(6), 707–716. https://doi.org/10.1080/07373937.2012.755541

Consoli, L., Dias, R. A. O., Carvalho, A. G. S., Silva, V. M., & Hubinger, M. D. (2019). Resveratrol-loaded microparticles: Assessing Maillard conjugates as encapsulating matrices. *Powder Technology, 353*, 247–256. https://doi.org/10.1016/j.powtec.2019.04.085

Drapala, K. P., Auty, M. A. E., Mulvihill, D. M., & O'Mahony, J. A. (2017). Influence of emulsifier type on the spray-drying properties of model infant formula emulsions. *Food Hydrocolloids, 69*, 56–66. https://doi.org/10.1016/j.foodhyd.2016.12.024

Gaffney, B. M., Havekotte, M., Jacobs, B., & Costa, L. (1996). Charm analysis of two citrus sinensis peel oil volatiles. *Perfumer & Flavorist, 21*, 1–5.

Giovanelli, G., Zanoni, B., Lavelli, V., & Nani, R. (2002). Water sorption, drying and antioxidant properties of dried tomato products. *Journal of Food Engineering, 52*(2), 135–141. https://doi.org/10.1016/S0260-8774(01)00095-4

Gouin, S. (2004). Microencapsulation: Industrial appraisal of existing technologies and trends. *Trends in Food Science and Technology, 15*(7–8), 330–347. https://doi.org/10.1016/j.tifs.2003.10.005

Goula, A. M., Adamopoulos, K. G., & Kazakis, N. A. (2004). Influence of spray drying conditions on tomato powder properties. *Drying Technology, 22*(5), 1129–1151. https://doi.org/10.1081/DRT-120038584

Goula, A. M., Karapantsios, T. D., Achilias, D. S., & Adamopoulos, K. G. (2008). Water sorption isotherms and glass transition temperature of spray dried tomato pulp. *Journal of Food Engineering, 85*(1), 73–83. https://doi.org/10.1016/j.jfoodeng.2007.07.015

Islam, M. Z., Kitamura, Y., Kokawa, M., Monalisa, K., Tsai, F.-H., & Miyamura, S. (2017). Effects of micro wet milling and vacuum spray drying on the physicochemical and antioxidant properties of orange (Citrus unshiu) juice with pulp powder. *Food and Bioproducts Processing, 101*, 132–144. https://doi.org/10.1016/j.fbp.2016.11.002

Islam, M. Z., Kitamura, Y., Yamano, Y., & Kitamura, M. (2016). Effect of vacuum spray drying on the physicochemical properties, water sorption and glass transition phenomenon of orange juice powder. *Journal of Food Engineering, 169*, 131–140. https://doi.org/10.1016/j.jfoodeng.2015.08.024

Jafari, S. M., Assadpoor, E., Bhandari, B., & He, Y. (2008). Nano-particle encapsulation of fish oil by spray drying. *Food Research International, 41*(2), 172–183. https://doi.org/10.1016/j.foodres.2007.11.002

Jansen-Alves, C., Maia, D. S. V., Krumreich, F. D., Crizel-Cardoso, M. M., Fioravante, J. B., da Silva, W. P., … Zambiazi, R. C. (2019). Propolis microparticles produced with pea protein: Characterization and evaluation of antioxidant and antimicrobial activities. *Food Hydrocolloids, 87*, 703–711. https://doi.org/10.1016/j.foodhyd.2018.09.004

King, C. J. (1995). Spray drying: Retention of volatile compounds revisited. *Drying Technology, 13*(5–7), 1221–1240. https://doi.org/10.1080/07373939508917018

Krokida, M. K., & Maroulis, Z. B. (1997). Effect of drying method on shrinkage and porosity. *Drying Technology, 15*(10), 2441–2458. https://doi.org/10.1080/07373939708917369

Kurozawa, L. E., Park, K. J., & Hubinger, M. D. (2009). Effect of maltodextrin and gum arabic on water sorption and glass transition temperature of spray dried chicken meat hydrolysate protein. *Journal of Food Engineering, 91*(2), 287–296. https://doi.org/10.1016/j.jfoodeng.2008.09.006

Lewicki, P. P. (1997). The applicability of the GAB model to food water sorption isotherms. *International Journal of Food Science and Technology, 32*(6), 553–557. https://doi.org/10.1111/j.1365-2621.1997.tb02131.x

Lomauro, C. J., Bakshi, A. S., & Labuza, T. P. (1985). Evaluation of food moisture sorption isotherm equations. Part I: Fruit, vegetable and meat products. *LWT – Food Science and Technology, 18*(2), 111–117.

Nijdam, J. J., & Langrish, T. A. G. (2006). The effect of surface composition on the functional properties of milk powders. *Journal of Food Engineering, 77*(4), 919–925. https://doi.org/10.1016/j.jfoodeng.2005.08.020

Phisut, N. (2012). Spray drying technique of fruit juice powder: Some factors influencing the properties of product. *International Food Research Journal, 19*(4), 1297–1306.

Quispe-Condori, S., Saldaña, M. D. A., & Temelli, F. (2011). Microencapsulation of flax oil with zein using spray and freeze drying. *LWT – Food Science and Technology, 44*(9), 1880–1887. https://doi.org/10.1016/j.lwt.2011.01.005

Ramos, F. M., Oliveira, C. C. M., Soares, A. S. P., & Silveira Júnior, V. (2016). Assessment of differences between products obtained in conventional and vacuum spray dryer. *Food Science and Technology, Campinas, 36*(4), 724–729. https://doi.org/10.1590/1678-457x.09216

Ramos, F. M., Silveira Júnior, V., & Prata, A. S. (2019). Assessing the vacuum spray drying effects on the properties of orange essential oil microparticles. *Food and Bioprocess Technology, 12*(11), 1917–1927. https://doi.org/10.1007/s11947-019-02355-2

Ramos, F. M., Ubbink, J., Silveira Júnior, V., & Prata, A. S. (2019). Drying of maltodextrin solution in a vacuum spray dryer. *Chemical Engineering Research and Design, 146*, 78–86. https://doi.org/10.1016/j.cherd.2019.03.036

Reineccius, G. A. (2001). *Multiple-core encapsulation: The spray drying of food ingredients. In Microencapsulation of Food Ingredients* (pp. 151–185). Surrey, England: Leatherhead: Leatherhead Publishing.

Reineccius, G. A. (2004). The spray drying of food flavors. *Drying Technology, 22*(6), 1289–1324. https://doi.org/10.1081/DRT-120038731

Reineccius, G. A. (1988). Spray-Drying of Food Flavors. In *Flavor Encapsulation* (pp. 55–66). https://doi.org/10.1021/bk-1988-0370.ch007.

Roos, Y. (1993). Melting and glass transitions of low molecular weight carbohydrates. *Carbohydrate Research, 238*, 39–48. https://doi.org/10.1016/0008-6215(93)87004-C

Semyonov, D., Ramon, O., & Shimoni, E. (2011). Using ultrasonic vacuum spray dryer to produce highly viable dry probiotics. *LWT - Food Science and Technology, 44*(9), 1844–1852. https://doi.org/10.1016/j.lwt.2011.03.021

Shishir, M. R. I., & Chen, W. (2017). Trends of spray drying: A critical review on drying of fruit and vegetable juices. *Trends in Food Science and Technology, 65*, 49–67. https://doi.org/10.1016/j.tifs.2017.05.006

Silva, E. K., Azevedo, V. M., Cunha, R. L., Hubinger, M. D., & Meireles, M. A. A. (2016). Ultrasound-assisted encapsulation of annatto seed oil: Whey protein isolate versus modified starch. *Food Hydrocolloids, 56*, 71–83. https://doi.org/10.1016/j.foodhyd.2015.12.006

Sobel, R., Gundlach, M., & Su, C.-P. (2014). Novel concepts and challenges of flavor microencapsulation and taste modification. In *In Microencapsulation in the Food Industry* (pp. 421–442). https://doi.org/10.1016/b978-0-12-404568-2.00033-9

Tonon, R. V., Baroni, A. F., Brabet, C., Gibert, O., Pallet, D., & Hubinger, M. D. (2009). Water sorption and glass transition temperature of spray dried açai (Euterpe oleracea Mart.) juice. *Journal of Food Engineering, 94*(3–4), 215–221. https://doi.org/10.1016/j.jfoodeng.2009.03.009

Tonon, R. V., Grosso, C. R. F., & Hubinger, M. D. (2011). Influence of emulsion composition and inlet air temperature on the microencapsulation of flaxseed oil by spray drying. *Food Research Internacional, 44*(1), 282–289. https://doi.org/10.1016/j.foodres.2010.10.018

Turek, C., & Stintzing, F. C. (2013). Stability of essential oils: A review. *Comprehensive Reviews in Food Science and Food Safety, 12*(1), 40–53. https://doi.org/10.1111/crf3.2013.12.issue-110.1111/1541-4337.12006

Vora, J. D., Matthews, R. F., Crandall, P. G., & Cook, R. (1983). Preparation and Chemical Composition of Orange Oil Concentrates. *Journal of Food Science, 48*(4), 1197–1199. https://doi.org/10.1111/jfds.1983.48.issue-410.1111/j.1365-2621.1983.tb09190.x

Zakarlan, J. A., & King, C. J. (1982). Volatiles loss in the nozzle zone during spray drying of emulsions. *Industrial and Engineering Chemistry Process Design and Development, 21*(1), 107–113. https://doi.org/10.1021/i200016a019

Zobel, H. F. (1988). Molecules to Granules: A comprehensive starch review. *Starch - Stärke, 40*(2), 44–50. https://doi.org/10.1002/(ISSN)1521-379X10.1002/star.v40:210.1002/star.19880400203